ELASTO-PLASTIC ANALYSIS OF THICK CYLINDERS SUBJECTED TO INTERNAL ELECTRO-MAGNETIC LOADING

H. Rajabi *

Department of Mechanical Engineering
Faculty of Engineering, Lahijan Branch
Islamic Azad University
Lahijan, Iran

A. Darvizeh

Department of Mechanical Engineering
Faculty of Engineering, Bandar Anzali Branch
Islamic Azad University
Bandar Anzali, Iran

ABSTRACT

A study of elasto-plastic deformation of circular cylindrical shells subjected to internal electro-magnetic forces is presented in this paper. The five governing equations in terms of resultant forces and resultant moments with respect to basic displacement vector components u, v and w are used. Theoretical formulations, based on the first-order shear deformation theory (FSDT), take into consideration transverse shear deformation and rotary inertia. The deformation theory of plasticity is employed for constitutive equations. The cylinders are composed of an elastic-plastic material with the von Mises yield criteria and non-linear plastic behaviour. Galerkin method is employed to convert the partial differential equations (PDEs) to ordinary differential equations (ODEs). The Newmark family of methods is used to numerically time integration of system of coupled second order ODEs. In order to prove the validity of the presented method and the solving process, the results obtained with the present analysis are compared with a set of available data. Good agreement observed between the results of the two approaches. Certainly, the aim of this paper is to create a more reliable and precise mathematical model of hollow-cylinders to avoid performing several experiments.

Keywords: Elasto-plastic deformation, Circular cylinder, Galerkin method, Deformation theory of plasticity, Dynamic force.

1. INTRODUCTION

Nowadays, methods which provide productive usage of material and energy sources and minimize problems encountered in the formation of metals are gaining great importance (Yasar *et al.* [1]). High velocity loading methods, such as electro-magnetic loading, electro-hydraulic loading, explosive loading, *etc*., are the examples of these methods.

Electromagnetic loading is the only high velocity loading technique to gain significant acceptance in commercial metal working (Tamhane *et al.* [2]). Electro-magnetic loading is a process where a pulsed magnetic field is used to processing metals with high electrical conductivity within a few microseconds. In this technique a high current pulse from a capacitor bank is passed through a coil or solenoid that is placed near a metallic conductor. The current pulse causes a high magnetic field around the coil. This field induces an eddy current in the workpiece and an associated secondary magnetic field. The two fields are repulsive and the force of magnetic repulsion causes deformation of the workpiece.

Although, the electro-magnetic forming (EMF) technique is widely used, there are a few works which attempt to study the effects of various parameters on its performance. The EMF process was first described by Boulger and Wagner [3]. The fundamental equations governing the process were derived from a series of comparative studies of analytical results and experimental data (Birdsall *et al.* [4]; Kegg and Haverbeck [5]; Baines *et al.* [6]). A number of simple and accurate approximate formulations have been suggested by Darvizeh [7,8]. The effects of some electrical and geometrical parameters have been investigated in these works.

* Corresponding author (harajabi@hotmail.com)

DOI : 10.1017/jmech.2012.51
Copyright © 2012 The Society of Theoretical and Applied Mechanics, R.O.C.
https://doi.org/10.1017/jmech.2012.51 Published online by Cambridge University Press

In recent years, finite element models of metallic plates and shells have been developed to study the EMF process (Murakoshi *et al.* [9]; Fenton and Daehn [10]; Oliveira *et al.* [11]; Yu *et al.* [12]; Yu and Li [13]; Rott *et al.* [14]).

In the present work, particular attention is devoted to modeling of thick circular cylindrical shells under internal electro-magnetic loading using an analytical solution. The word "thick" means that the effect of the factor $(1 + z/R)$ is considered in calculating resultant forces and resultant moments. This factor results from the trapezoid-like shape of the cross-section of the shell and is usually neglected in the thin shell theory (Mao and Lu [15]). Theoretical formulations, based on FSDT, take into consideration transverse shear deformation and rotary inertia effects. The formulation is general. Different boundary conditions, host shell materials (which may be isotropic and orthotropic), ratios of the thickness of the host shell and piezoelectric layers, order of shear deformation theories and even forms of assumed solutions can be easily accommodated into analysis. The von Mises yield criteria is implemented to predict the elastic or plastic deformation of the cylinder material during the loading process. In this case, the Ramberg-Osgood nonlinear stress- strain relation is used to describe the material behaviour in the plastic zone. Galerkin method is used to convert the partial differential equations (PDEs) to ordinary differential equations (ODEs). The Newmark family of methods is used to numerically time integration of system of coupled second order ordinary differential equations (ODEs). In order to prove the validity of the presented method and the solving process, a dynamic numerical solution for the same example is used. Comparing the results of the presented method with those obtained with the numerical solution, it can be found that the presented method is effective and accurate. The materials used in the present work are selected to investigate the influence of the material properties on the elastic-plastic behaviour of the shell.

The aim of this paper is to find a more precise and predictive model to avoid performing multiple experiments. The results of this paper can serve as a reference for future study in the design of engineering structures.

2. GOVERNING EQUATIONS

2.1 Equations of Motion

A three-dimensional elastic body enclosed by two neighborhood or closely curved surfaces called "shell". The distance between these two surfaces defines the thickness of the shell. The "mid-surface" of the shell is a surface passing through the mid-thickness at each point (Farshad [16]). It means that, in a circular cylinder of radius R the mid-surface is a minimal surface with the radii of curvature R and infinite along the radial and axial directions, respectively. If the thickness of the shell is small compared with the other dimensions, then the shell is considered as a "thin" one; otherwise, the shell is "thick".

Consider a thick-walled circular cylindrical shell made up of a linear orthotropic material (Fig. 1). The orthogonal coordinate system (x, ϑ, z) is fixed at the mid-surface of the tube with length L, thickness H, and radius R. x is the axial direction, ϑ is the circumferential direction and z is the radial direction. The deformations of the tube are defined by u, v, w which are displacements of the point in x, ϑ, z.

The stress analysis on the sides of an element of the shell structure is shown in Fig. 2. For the mid-surface, we defined the six force (N_x, N_ϑ, $N_{x\vartheta}$, $N_{\vartheta x}$, Q_x, Q_ϑ) and four moment (M_x, M_ϑ, $M_{x\vartheta}$, $M_{\vartheta x}$) resultants and the distributed load consisting of three forces (P_x, P_ϑ, P_z) and two moments (m_x, m_ϑ). The governing equations of motion in the longitudinal, tangential and radial directions in terms of the force and moment resultants are as follows (Darvizeh and Darvizeh [17])

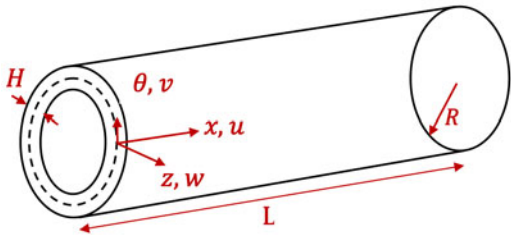


Fig. 1 Circular cylindrical shell in polar coordinate system, x, ϑ, z directions and u, v, w displacements

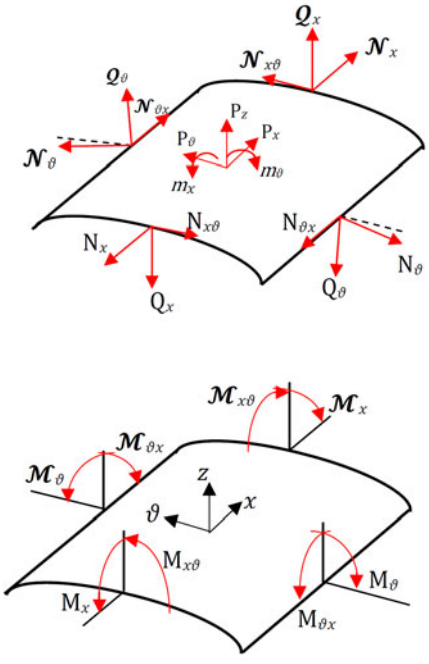


Fig.2 The forces and moments acting on the sides of an element of the circular cylindrical shell

https://doi.org/10.1017/jmech.2012.51 Published online by Cambridge University Press

$$
\begin{aligned}
&N_{x,x}+\frac{N_{\vartheta x,\vartheta}}{R}+P_x = I_0\,\ddot{u}_0 + I_1\,\ddot{\varphi}_x\ ,\\
&N_{x\vartheta,x}+\frac{N_{\vartheta,\vartheta}}{R}+\frac{Q_\vartheta}{R}+P_\vartheta = I_0\,\ddot{v}_0 + I_1\,\ddot{\varphi}_\vartheta\ ,\\
&Q_{x,x}+\frac{Q_{\vartheta,\vartheta}}{R}-\frac{N_\vartheta}{R}+P_z = I_0\,\ddot{w}_0\ ,\\
&M_{x,x}+\frac{M_{\vartheta x,\vartheta}}{R}-Q_x+M_x = I_1\,\ddot{u}_0 + I_2\,\ddot{\varphi}_x\ ,\\
&M_{x\vartheta,x}+\frac{M_{\vartheta,\vartheta}}{R}-Q_\vartheta+m_\vartheta = I_1\,\ddot{v}_0 + I_2\,\ddot{\varphi}_\vartheta\ ,
\end{aligned}
\tag{1}
$$

the mass moments of inertia are

$$
\begin{aligned}
I_0 &= \int_{-\frac{H}{2}}^{\frac{H}{2}} \rho\left(1+\frac{z}{R}\right)dz\ ,\\
I_1 &= \int_{-\frac{H}{2}}^{\frac{H}{2}} \rho\, z\left(1+\frac{z}{R}\right)dz\ ,\\
I_2 &= \int_{-\frac{H}{2}}^{\frac{H}{2}} \rho\, z^2\left(1+\frac{z}{R}\right)dz\ ,
\end{aligned}
\tag{2}
$$

and ρ is the density of the shell.

The force and moment resultants that act on a shell element are defined as the force and moment per unit length of the shell's mid-surface. The resultants, which are obtained by integrating the stresses acting on differential area elements of a shell element, have the following definitions

$$
\begin{aligned}
N_x &= \int_{-\frac{H}{2}}^{\frac{H}{2}} \sigma_x\left(1+\frac{z}{R}\right)dz\ ,\\
N_\vartheta &= \int_{-\frac{H}{2}}^{\frac{H}{2}} \sigma_\vartheta\, dz\ ,\\
N_{x\vartheta} &= \int_{-\frac{H}{2}}^{\frac{H}{2}} \sigma_{x\vartheta}\left(1+\frac{z}{R}\right)dz\ ,\\
N_{\vartheta x} &= \int_{-\frac{H}{2}}^{\frac{H}{2}} \sigma_{\vartheta x}\, dz\ ,\\
M_x &= \int_{-\frac{H}{2}}^{\frac{H}{2}} \sigma_x\left(1+\frac{z}{R}\right)z\, dz\ ,\\
M_\vartheta &= \int_{-\frac{H}{2}}^{\frac{H}{2}} \sigma_\vartheta\, z\, dz\ ,\\
M_{x\vartheta} &= \int_{-\frac{H}{2}}^{\frac{H}{2}} \sigma_{x\vartheta}\left(1+\frac{z}{R}\right)z\, dz\ ,\\
M_{\vartheta x} &= \int_{-\frac{H}{2}}^{\frac{H}{2}} \sigma_{\vartheta x}\, z\, dz\ ,\\
Q_x &= \int_{-\frac{H}{2}}^{\frac{H}{2}} \sigma_{zx}\left(1+\frac{z}{R}\right)dz\ ,\\
Q_\vartheta &= \int_{-\frac{H}{2}}^{\frac{H}{2}} \sigma_{\vartheta z}\, dz\ ,
\end{aligned}
\tag{3}
$$

where σ_x, σ_ϑ, $\sigma_{x\vartheta}$, σ_{zx} and $\sigma_{\vartheta z}$ are the normal and shear stresses distributed in the shell.

Note that, for thick shell the term (z/R) in the force and moment resultants is so large that it cannot be neglected.

2.2 Plastic Constitutive Equations

In this section, the deformation theory of plasticity is used to relate stresses and strains. According to the deformation theory of plasticity, the relation between the stress tensor σ_{ij} and the plastic strain tensor ε_{ij} can be written as

$$
\varepsilon_{ij} = \frac{3}{2E_s}\sigma_{ij} - \left(\frac{1}{2E_s}-\frac{1-2v}{3E}\right)\sigma_{kk}\ \delta_{ij} \tag{4}
$$

where E and υ are Young's modulus and Poisson's ration. E_s, which is called secant modulus, is the slop of a line from the origin to any point on the stress-strain curve and can be defined as

$$
E_s = \frac{\sigma_e}{\varepsilon_e}\ . \tag{5}
$$

σ_e and ε_e are the effective stress and strain, respectively.

Now, using Eq. (4), we can express the constitutive equations into the following form

$$
\begin{pmatrix}\sigma_x\\ \sigma_\theta\\ \sigma_z\\ \tau_{\theta z}\\ \tau_{xz}\\ \tau_{x\theta}\end{pmatrix} = \begin{pmatrix} Q_{11} & Q_{12} & Q_{13} & 0 & 0 & 0\\ Q_{21} & Q_{22} & Q_{23} & 0 & 0 & 0\\ Q_{31} & Q_{32} & Q_{33} & 0 & 0 & 0\\ 0 & 0 & 0 & Q_{44} & 0 & 0\\ 0 & 0 & 0 & 0 & Q_{55} & 0\\ 0 & 0 & 0 & 0 & 0 & Q_{66}\end{pmatrix}\begin{pmatrix}\varepsilon_x\\ \varepsilon_\theta\\ \varepsilon_z\\ \gamma_{\theta z}\\ \gamma_{xz}\\ \gamma_{x\theta}\end{pmatrix}, \tag{6}
$$

the parameters in the above equation, are

$$
\begin{aligned}
&Q_{11} = Q_{22} = Q_{33} = \frac{3E+4E_s(1-2v)}{9(1-2v)}\ ,\\
&Q_{12} = Q_{21} = Q_{13} = Q_{31} = Q_{23} = Q_{32} = \frac{3E+2E_s(1-2v)}{9(1-2v)}\ ,\\
&Q_{44} = Q_{55} = Q_{66} = \frac{2E_s}{3}\ .
\end{aligned}
\tag{7}
$$

2.3 Compatibility Equations

The strain-displacement equations for a thick cylindrical shell are given by Eq. (8)

$$
\begin{aligned}
&\varepsilon_x = u_{,x}\ ,\\
&\varepsilon_\vartheta = (v_{,\vartheta}+w)/(R+z)\ ,\\
&\varepsilon_z = w_{,z}\ ,\\
&\gamma_{\vartheta z} = (w_{,\vartheta}-v)/(R+z)+\varphi_\vartheta\ ,\\
&\gamma_{xz} = \varphi_x + w_{,x}\ ,\\
&\gamma_{x\vartheta} = u_{,\vartheta}/(R+z)+v_{,x}\ ,
\end{aligned}
\tag{8}
$$

As mentioned before, u, v, w are the displacements along x, ϑ, z axes respectively; φ_x and φ_ϑ are angles of rotations of the cross-sections that were normal to the mid-surface of the unformed shell.

First order theory is used to deal with the influence of shear forces on the deformation of the shell. In the first order shear deformation Kirchhoff hypothesis is relaxed by not constraining the transverse normals to remain perpendicular to the mid-surface after deformation. This amounts to including transverse shear

https://doi.org/10.1017/jmech.2012.51 Published online by Cambridge University Press

strains in the theory. The inextensibility of transverse normals requires that w be independent of the thickness coordinate.

According to the first order shear deformation theory, the displacement fields are of the form

$$\begin{aligned} u(x,\vartheta,z,t) &= u_0(x,\vartheta,t) + z\varphi_x(x,\vartheta,t)\,, \\ v(x,\vartheta,z,t) &= v_0(x,\vartheta,t) + z\varphi_\vartheta(x,\vartheta,t)\,, \\ w(x,\vartheta,z,t) &= w_0(x,\vartheta,t)\,, \end{aligned} \tag{9}$$

where u_0, v_0, w_0, φ_x and φ_ϑ are unknowns to be determined.

In fact, u_0, v_0, w_0, φ_x and φ_ϑ are the displacements of a point on the surface $z = 0$ and the rotations of transverse normal about its ϑ and x axis respectively.

Substituting Eq. (9) into Eq. (8) gives

$$\begin{aligned} &\varepsilon_x = u_{0,x} + z\,\varphi_{x,x}\,, \\ &\varepsilon_\vartheta = (v_{0,\vartheta} + z\,\varphi_{\vartheta,\vartheta} + w_0)/(R+z)\,, \\ &\varepsilon_z = 0\,, \\ &\gamma_{\vartheta z} = (w_{0,\vartheta} - v_0 - z\varphi_\vartheta)/(R+z) + \varphi_\vartheta\,, \\ &\gamma_{xz} = \varphi_x + w_{0,x}\,, \\ &\gamma_{x\vartheta} = (u_{0,\vartheta} + z\,\varphi_{x,\vartheta})/(R+z) + v_{0,x} + z\,\varphi_{\vartheta,x}\,, \end{aligned} \tag{10}$$

Using expressions (10), (6) and (3) in Eq. (1), yield the following equations of motion in terms of the displacements and their corresponding derivatives

$$\begin{aligned} &\left(A_{11}+\frac{B_{11}}{R}\right)u_{0,xx} + \left(\frac{A_{66}}{R^2} - \frac{B_{66}}{R^3} + \frac{C_{66}}{R^4}\right)u_{0,\vartheta\vartheta} + \left(\frac{A_{12}}{R}+\frac{A_{66}}{R}\right)v_{0,x\vartheta} + \left(\frac{A_{12}}{R}\right)w_{0,x} \\ &+\left(B_{11}+\frac{C_{11}}{R}\right)\varphi_{x,xx} + \left(\frac{B_{66}}{R^2} - \frac{C_{66}}{R^3} + \frac{D_{66}}{R^4}\right)\varphi_{x,\vartheta\vartheta} + \left(\frac{B_{12}}{R}+\frac{B_{66}}{R}\right)\varphi_{\vartheta,x\vartheta} + P_x = I_0\,\ddot{u}_0 + I_1\,\ddot{\varphi}_x\,, \\ &\left(\frac{A_{12}}{R}+\frac{A_{66}}{R}\right)u_{0,x\vartheta} - \left(\frac{A_{44}}{R^2} - \frac{B_{44}}{R^3} + \frac{C_{44}}{R^4}\right)v_0 + \left(A_{66}+\frac{B_{66}}{R}\right)v_{0,xx} + \left(\frac{A_{22}}{R^2} - \frac{B_{22}}{R^3} + \frac{C_{22}}{R^4}\right)v_{0,\vartheta\vartheta} \\ &+\left(\frac{A_{22}}{R^2} + \frac{A_{44}}{R^2} - \frac{B_{22}}{R^3} - \frac{B_{44}}{R^3} + \frac{C_{22}}{R^4} + \frac{C_{44}}{R^4}\right)w_{0,\vartheta} + \left(\frac{B_{12}}{R}+\frac{B_{66}}{R}\right)\varphi_{x,x\vartheta} + \left(\frac{A_{44}}{R} - \frac{B_{44}}{R^2} + \frac{C_{44}}{R^3}\right)\varphi_\vartheta \\ &+\left(B_{66}+\frac{C_{66}}{R}\right)\varphi_{\vartheta,xx} + \left(\frac{B_{22}}{R^2} - \frac{C_{22}}{R^3} + \frac{D_{22}}{R^4}\right)\varphi_{\vartheta,\vartheta\vartheta} + P_\vartheta = I_0\,\ddot{v}_0 + I_1\,\ddot{\varphi}_\vartheta\,, \\ &\left(\frac{A_{12}}{R}\right)u_0 + \left(\frac{A_{22}}{R^2} + \frac{A_{44}}{R^2} - \frac{B_{22}}{R^3} - \frac{B_{44}}{R^3} + \frac{C_{22}}{R^4} + \frac{C_{44}}{R^4}\right)v_{0,\vartheta} + \left(\frac{A_{22}}{R^2} - \frac{B_{22}}{R^3} + \frac{C_{22}}{R^4}\right)w_0 - \left(A_{55}+\frac{B_{55}}{R}\right)w_{0,xx} \\ &-\left(\frac{A_{44}}{R^2} - \frac{B_{44}}{R^3} + \frac{C_{44}}{R^4}\right)w_{0,\vartheta\vartheta} - \left(A_{55} - \frac{B_{12}}{R} + \frac{B_{55}}{R}\right)\varphi_{x,x} - \left(\frac{A_{44}}{R} - \frac{B_{22}}{R^2} - \frac{B_{44}}{R^2} + \frac{C_{22}}{R^3} + \frac{C_{44}}{R^3} - \frac{D_{22}}{R^4}\right)\varphi_{\vartheta,\vartheta} + P_z = I_0\,\ddot{w}_0\,, \\ &\left(B_{11}+\frac{C_{11}}{R}\right)u_{0,xx} + \left(\frac{B_{66}}{R^2} - \frac{C_{66}}{R^3} + \frac{D_{66}}{R^4}\right)u_{0,\vartheta\vartheta} + \left(\frac{B_{12}}{R}+\frac{B_{66}}{R}\right)v_{0,x\vartheta} - \left(A_{55} - \frac{B_{12}}{R} + \frac{B_{55}}{R}\right)w_{0,x} \\ &-\left(A_{55}+\frac{B_{55}}{R}\right)\varphi_x + \left(C_{11}+\frac{D_{11}}{R}\right)\varphi_{x,xx} + \left(\frac{C_{66}}{R^2} - \frac{D_{66}}{R^3} + \frac{E_{66}}{R^4}\right)\varphi_{x,\vartheta\vartheta} + \left(\frac{C_{12}}{R}+\frac{C_{66}}{R}\right)\varphi_{\vartheta,x\vartheta} + m_x = I_1\,\ddot{u}_0 + I_2\,\ddot{\varphi}_x\,, \\ &\left(\frac{B_{12}}{R}+\frac{B_{66}}{R}\right)u_{0,x\vartheta} - \left(\frac{A_{44}}{R^2} - \frac{B_{44}}{R^3} + \frac{C_{44}}{R^4}\right)v_0 + \left(B_{66}+\frac{C_{66}}{R}\right)v_{0,xx} + \left(\frac{B_{22}}{R^2} - \frac{C_{22}}{R^3} + \frac{D_{22}}{R^4}\right)v_{0,\vartheta\vartheta} \\ &-\left(\frac{A_{22}}{R} - \frac{B_{44}}{R^2} - \frac{B_{44}}{R^2} + \frac{C_{22}}{R^3} + \frac{C_{44}}{R^3} - \frac{D_{22}}{R^4}\right)w_{0,\vartheta} + \left(\frac{C_{12}}{R}+\frac{C_{66}}{R}\right)\varphi_{x,x\vartheta} - \left(A_{44} - \frac{B_{44}}{R} + \frac{C_{44}}{R^2}\right)\varphi_\vartheta \\ &+\left(C_{66}+\frac{D_{66}}{R}\right)\varphi_{\vartheta,xx} + \left(\frac{C_{22}}{R^2} - \frac{D_{22}}{R^3} + \frac{E_{22}}{R^4}\right)\varphi_{\vartheta,\vartheta\vartheta} + m_\vartheta = I_1\,\ddot{v}_0 + I_2\,\ddot{\varphi}_\vartheta\,, \end{aligned} \tag{11}$$

where

$$\begin{aligned} A_{ij} &= \int_{-\frac{H}{2}}^{\frac{H}{2}} K_{ij}^2\,Q_{ij}\,dz\,, \\ B_{ij} &= \int_{-\frac{H}{2}}^{\frac{H}{2}} K_{ij}^2\,Q_{ij}\,z\,dz\,, \\ C_{ij} &= \int_{-\frac{H}{2}}^{\frac{H}{2}} K_{ij}^2\,Q_{ij}\,z^2\,dz\,, \\ D_{ij} &= \int_{-\frac{H}{2}}^{\frac{H}{2}} K_{ij}^2\,Q_{ij}\,z^3\,dz\,, \\ E_{ij} &= \int_{-\frac{H}{2}}^{\frac{H}{2}} K_{ij}^2\,Q_{ij}\,z^4\,dz\,. \end{aligned}$$

https://doi.org/10.1017/jmech.2012.51 Published online by Cambridge University Press

And $K_{ij} = 1$ except for K_{44}, K_{55}. The shear correction factors are taken as $K_{44} = K_{55} = \sqrt{\frac{5}{6}}$. (Jonnalaggada *et al.* [18])

2.4 Galerkin Method

In this section the Galerkin method has been used to convert PDEs to ODEs. The boundary conditions for simply supported cylindrical shell are

$$x = 0, L : v_0 = w_0 = \varphi_\vartheta = N_x = M_x = 0 . \tag{12}$$

Thus, the displacement field, which satisfy the boundary conditions, can be written as

$$\begin{aligned} u_o(x,\vartheta,t) &= U_0(t) f_1(x,\vartheta) , \\ v_o(x,\vartheta,t) &= V_0(t) f_2(x,\vartheta) , \\ w_o(x,\vartheta,t) &= W_0(t) f_3(x,\vartheta) , \\ \varphi_x(x,\vartheta,t) &= \varphi_{x0}(t) f_1(x,\vartheta) , \\ \varphi_\vartheta(x,\vartheta,t) &= \varphi_{\vartheta 0}(t) f_2(x,\vartheta) , \end{aligned} \tag{13}$$

where

$$\begin{aligned} f_1(x,\vartheta) &= \cos \alpha x \cos \beta \vartheta , \\ f_2(x,\vartheta) &= \sin \alpha x \sin \beta \vartheta , \\ f_3(x,\vartheta) &= \sin \alpha x \cos \beta \vartheta , \\ \alpha &= \frac{m\pi}{L} , \\ \beta &= \frac{n\pi}{\varphi} . \end{aligned}$$

$U_0(t)$, $V_0(t)$, $W_0(t)$, $\varphi_{x0}(t)$ and $\varphi_{\vartheta 0}(t)$ are the time dependent components of the displacement fields.

The weighted integral statement of the Galerkin method is written as

$$\begin{aligned} &\int_0^{2\pi}\int_0^L (L_{11}u_0 + L_{12}v_0 + L_{13}w_0 + L_{14}\varphi_x + L_{15}\varphi_\vartheta + P_x - I_0\ddot{u}_0 - I_1\ddot{\varphi}_x)\,\delta u_0\, dxd\theta = 0 , \\ &\int_0^{2\pi}\int_0^L (L_{21}u_0 + L_{22}v_0 + L_{23}w_0 + L_{24}\varphi_x + L_{25}\varphi_\vartheta + P_\vartheta - I_0\ddot{u}_0 - I_1\ddot{\varphi}_x)\,\delta v_0\, dxd\theta = 0 , \\ &\int_0^{2\pi}\int_0^L (L_{31}u_0 + L_{32}v_0 + L_{33}w_0 + L_{34}\varphi_x + L_{35}\varphi_\vartheta + P_z - I_0\ddot{w}_0)\,\delta w_0\, dxd\theta = 0 , \\ &\int_0^{2\pi}\int_0^L (L_{41}u_0 + L_{42}v_0 + L_{43}w_0 + L_{44}\varphi_x + L_{45}\varphi_\vartheta + m_x - I_1\ddot{u}_0 - I_2\ddot{\varphi}_x)\,\delta\varphi_x\, dxd\theta = 0 , \\ &\int_0^{2\pi}\int_0^L (L_{51}u_0 + L_{52}v_0 + L_{53}w_0 + L_{54}\varphi_x + L_{55}\varphi_\vartheta + m_\vartheta - I_1\ddot{v}_0 - I_2\ddot{\varphi}_\vartheta)\,\delta\varphi_\vartheta\, dxd\theta = 0 . \end{aligned} \tag{14}$$

Substituting Eq. (13) into Eq. (14) and performing the integration, we obtain the following matrix equation

$$[M]\{\ddot{U}\} + [K]\{U\} = \{P\} , \tag{15}$$

where $[M]$, $[K]$ are the inertia and stiffness matrices and $\{\ddot{U}\}$, $\{U\}$, $\{P\}$ are the acceleration, displacement and load vectors. The coefficients of matrix K are very complicated. They are computed using Maple software and not presented here.

3. TIME INTEGRATION

The Newmark family of methods is used in the present study to numerically time integration of the system of five coupled second order ODEs. The recursive relation among displacements, velocities at times t and $t + \Delta t$ are:

$$u^{t+\Delta t} = u^t + \Delta t \dot{u}^{\,t} + \frac{\Delta t^2}{2}\left[(1-2\beta)\ddot{u}^{\,t} + 2\beta\ddot{u}^{\,t+\Delta t}\right], \tag{16}$$

$$\dot{u}^{t+\Delta t} = \dot{u}^t + \Delta t\left[(1-\gamma)\ddot{u}^{\,t} + \gamma\ddot{u}^{\,t+\Delta t}\right]. \tag{17}$$

The Newmark's parameters are chosen to be $\beta = 1/4$ and $\gamma = 1/2$. By setting these parameters, it results in the constant acceleration scheme, which is desirable because of its second order accuracy and non-dissipative nature.

4. ELECTRO-MAGNETIC FORMING (EMF)

Although, high velocity loading methods have many attractive characteristics, there are a few experiments. In high velocity loading process it is very difficult to control the energy and to make parts with complicated

https://doi.org/10.1017/jmech.2012.51 Published online by Cambridge University Press

shapes. Therefore, it is very important to establish a mathematical model of shells or plates under these kinds of loads. In the last years, due to multiple advantages, EMF has been used in many industrial sectors such as automotive, aerospace, and defence.

In the EMF process the high current pulse in the coil produces a high transient magnetic field about it. The change in this field induces an eddy current in the workpiece. The fields around the workpiece and coil are repulsive and as a result they repel each other. The schematic diagram of the tube expansion experiment is shown in Fig. 3. As shown in this figure, the setup consists of a capacitor bank of capacitance C connected to a coil that is placed coaxially and symmetrically inside a tube. 'r_c' and 'r_w' are the effective radius of the coil and tube, respectively. Materials with high electrical conductivity and low yield stress, such as copper, aluminum and brass can be formed very easily (Al-Hassani *et al.* [19]); forming of mild steel is less efficient and stainless steel can only be formed by special techniques (James and Philpott [20]).

In this paper, in order to obtain the electro-magnetic pressure function, we use the simple and accurate approximate formulations given by Darvizeh (Darvizeh [7]).

The actual magnetic forming circuit is quite closely represented by the circuit diagram in Fig. 4. The coil has a resistance R_c, an inductance L_c and is coupled by a mutual inductance M with the workpiece which has a resistance and inductance R_w and L_w, respectively.

For the conditions which apply in magnetic forming, the discharge current i can be studied by considering the equivalent circuit, Fig. 4, in which the equivalent parameters R_e and L_e can be written as

$$L_e = L_c\left(1-\frac{r_c^2}{r_w^2}\right), \tag{18}$$

$$R_e = R_c + \frac{2\pi\, r_w\, L\, \rho\, N^2}{\delta}\left(\frac{r_c}{r_w}\right)^4, \tag{19}$$

where

$$\delta = \sqrt{\frac{2\rho}{\mu_0\, \mu\omega}}. \tag{20}$$

δ, which is called "skin depth", is a property of a material which dictates to what extent an electromagnetic wave can penetrate the material. ρ is the electric resistance coefficient of the workpiece, μ denotes the permeability of the respective material, μ_0 is the vacuum permeability, ω is the angular frequency of the magnetic flux density and N is the turn number on the unit length of coil. Also, r_c and r_w are the effective radius of the coil and the effective radius of the workpiece, respectively.

In the equivalent circuit, the current is proximately expressed by

$$i = -\frac{E_0}{L_e\,\omega}e^{-\frac{R_e t}{2L_e}}\sin\omega t. \tag{21}$$

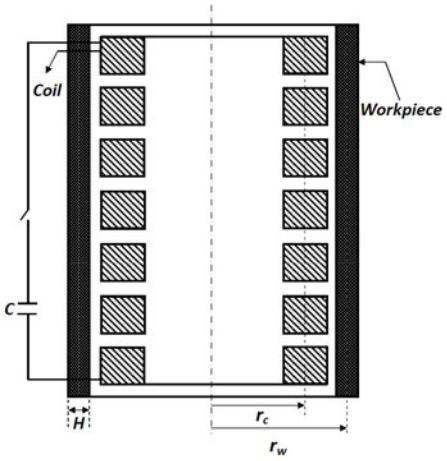


Fig. 3 Schematic diagram of the experimental tubular workpiece bulging set-up

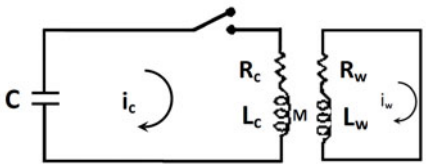


Fig. 4 Line circuit diagram primary and secondary circuits

The magnetic pressure is calculated by

$$P_{EM} = \frac{1}{2}\mu\,\mu_0\, N^2\left(\frac{r_c}{r_w}\right)^4 - \frac{E_0^2 C}{L_e}e^{-\frac{R_e t}{L_e}}\sin^2\omega t. \tag{22}$$

5. RESULTS & DISCUSSION

A numerical study is carried out to assess the accuracy of the presented method and the solving process. The radial displacement of a circular cylindrical shell, with simply supported edges (mechanical dof's) is calculated. The material properties of the shell of aluminium are listed in Table 1. The length and the radius of the shell are equal to 140mm and 25mm, respectively. Moreover, the ratio of the thickness, defined as $S = R/H$, is about 20.

The von Mises yield criterion is given by

$$f = \sigma_e - \sigma_y. \tag{23}$$

According to the von-Mises yield criterion, yielding occurs when the effective stress becomes equal to the yield stress, *i.e.* yield occurs when

$$f = 0. \tag{24}$$

The Ramberg-Osgood equation, which is used to model the material behaviour in the plastic zone, can be expressed by

$$\varepsilon = \frac{\sigma}{E} + \alpha\frac{\sigma_y}{E}\left(\frac{\sigma}{\sigma_y}\right)^n, \tag{25}$$

https://doi.org/10.1017/jmech.2012.51 Published online by Cambridge University Press

where α and n are Ramberg-Osgood parameters, and are obtained from experimental tests.

The pressure acting on the cylinder surface has been plotted in Fig. 5. Figure 6 gives the radial displacement along the half length of the tube, for different time steps. As illustrated in this figure, the radial displacement at the ends is zero. Also, the maximum radial displacement at the centre is larger than at the other nodes, in all steps. The radius of the cylinder increases rapidly and the deformation finishes in a very short time (at 150μs in this case). In Fig. 6, the theoretical displacement curves are compared with the numerical results reported by Zhong *et al.* [21]. It is can be seen that a good agreement stands between the theoretical results and numerical data.

The two dimensional (2D) axisymmetric representation of the cylinder after deformation is given in Fig. 7, showing the position five nodes on the tube. The variation of the radial displacements versus time for each node is demonstrated in Fig. 8. The elasto- plastic deformation of the cylinder due to the elector- magnetic loading is shown in this figure. The figure also describes the vibration behaviour of the structure. It is depicted that, after the plastic deformation process, the cylinder vibrates around the maximum value of plastic displacement.

Table 1 Material properties of the shell

Material	Mass density (kg/m^3)	Young modulus (GPa)	Poisson's ratio
Aluminium	2.80×10^3	70	0.33

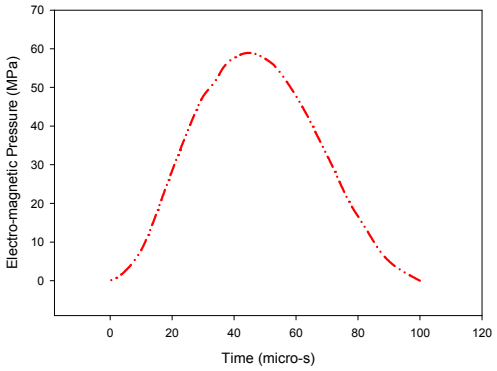


Fig. 5 Variation of radial pressure versus time

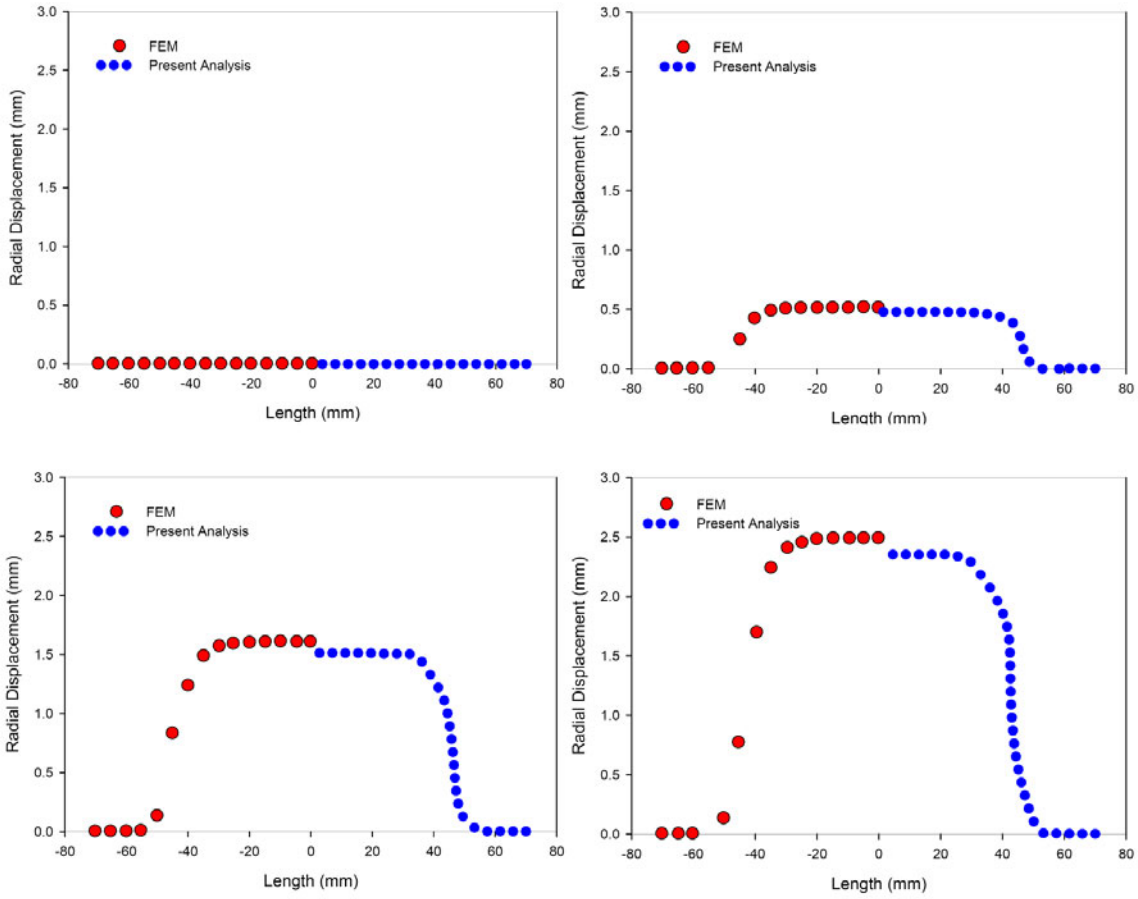


Fig. 6 The different time steps in the forming process. Comparison of the results of the presented analysis with numerical data after 0, 50, 75 and 150 micro-seconds

https://doi.org/10.1017/jmech.2012.51 Published online by Cambridge University Press

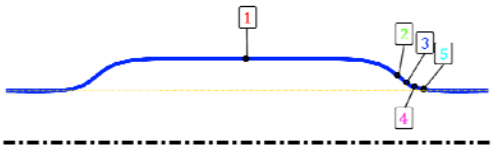


Fig. 7 The deformed cylinder and five nodes on it

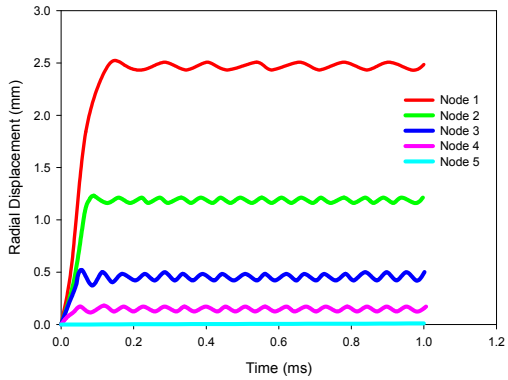


Fig. 8 The radial displacements versus time for each node

6. CONCLUSIONS

A thick shell theory with the FSDT is used to analyze the expansion of an aluminium tube. The constitutive equations are based on the deformation theory of plasticity. The material is assumed to exhibit a nonlinear strain-hardening behaviour. Comparison of theoretical and numerical results shows that the presented model correctly predicts the plastic deformation of cylinders. Therefore, this analysis is suitable for quick and accurate design purposes. The major aim of this paper is to create a simple and accurate model of thick cylinders to avoid performing several experiments.

REFERENCES

1. Yasar, M., Demirci, H. I. and Kadib, I., "Detonation Forming of Aluminium Cylindrical Cups Experimental and Theoretical Modeling," *Materials & Design*, **27**, pp. 397–404 (2006).
2. Tamhane, A. A., Padmanabhan, M., Fenton, G., Altynova, M. and Daehn, G. S., "Opportunities in High-Velocity Forming of Sheet Metal," *Metalforming Magazine*, January (1997).
3. Boulger, F. W. and Wagner, H. J., "High Velocity Metal Working Processes Based on the Sudden Release of Electrical Energy," *Defense Metals Information Center*, Battelle Memorial Institute (1960).
4. Birdsall, D. H., Ford, F. C., Furth, H. P. and Riley, R. E., "Magnetic Forming," *American Machinist / Metalworking Manufacturing*, **105**, pp. 117–121 (1961).
5. Kegg, R. L. and Haverbeck, K., "Effect of Process Variables in Electric Discharge Forming," *Annals of the CIRP*, **11**, pp. 131–137 (1962).
6. Baines, K., Duncan, J. L. and Johnson, W., "Electromagnetic Metal Forming," *Proceedings of the Institution of Mechanical Engineers*, **180**, pp. 348–362 (1965).
7. Darvizeh, A., *Electro-Magnetic Metal Forming*. The University of Guilan Press (1991).
8. Darvizeh, A., "High Energy Rate Forming of Thin-Walled Tubes by Electro-Magnetic Forces," *Iranian Journal of Mechanical Engineering. Transaction of the ISME*, **2**, pp. 1–13 (1994).
9. Murakoshi, Y., Takahashi, M., Sano, T., Hanada, K. and Negishi, H., "Inside Bead Forming of Aluminum Tube by Electro-Magnetic Forming," *Journal of Material Processing Technology*, **80-81**, pp. 695–699 (1998).
10. Fenton, G. and Daehn, G. S., "Modeling of Electromagnetically Formed Sheet Metal," *Journal of Materials Processing Technology*, **75**, pp. 6–16 (1998).
11. Oliveira, D. A., Worswick, M. J., Finn, M. and Newman, D., "Electromagnetic Forming of Aluminum Alloy Sheet: Free-Form and Cavity Fill Experiments and Model," *Journal of Material Processing Technology*, **170**, pp. 350–362 (2005).
12. Yu, H. P., Li, Z. and Lee, C. F., "Numerical Simulation of Coupled Fields of Electromagnetic Forming for Tube Compression Based on FEM," *Chinese Journal of Mechanical Engineering*, **42**, pp. 231–234 (2006).
13. Yu, H. P. and Lee, C. F., "Effects of Coil Length on Tube Compression in Electromagnetic Forming," *The Transactions of Nonferrous Metals Society of China*, **17**, pp. 1270–1275 (2007).
14. Rott, M., Seidel, U., Streibl, B., Suttrop, W., Vierle, T. and The ASDEX Upgrade Team, "Electro-Magnetic Modeling of the Planned Active In-Vessel Coils at ASDEX Upgrade," *Fusion Engineering Design*, **84**, pp. 1653–1657 (2009).
15. Mao, R. and Lu, G., "A Study of Elastic-Plastic Buckling of Cylindrical Shells Under Torsion," *Thin-Walled Structures*, **40**, pp. 1051–1071 (2002).
16. Farshad, M., *Design and Analysis of Shell Structures*, Kluwer Academic Publishers (1992).
17. Darvizeh, A. and Darvizeh, M., *Stress Analysis in Thick Spherical and Cylindrical Shells*, The University of Guilan Press (1993).
18. Jonnalaggada, K. D., Blandford, G. E. and Tauchert, T. R., "Piezothermoelastic Composite Plate Analysis Using First-Order Shear Deformation Theory," *Computers and Structures*, **51**, pp. 79–89 (1994).
19. Al-Hassani, S. T. S., Duncan, J. L. and Johnson, W., "The Influence of Electrical and Geometrical Parameters in Magnetic Forming," *Proceedings of the 8th International MTDR Conference*, pp. 1333–1347 (1967).
20. James, T. E. and Philpott, J., "High Frequency Systems for Magnetic Forming of Resistive Materials," *Proceedings of the I.E.E Conference*, pp. 37–44 (1970).
21. Li, C. F., Yu, H. P. and Zhao, Z. H., "Effect of Tube Size on Electromagnetic Tube Bulging," *The Transactions of Nonferrous Metals Society of China*, **17**, pp. 705–710 (2007).

(Manuscript received July 10, 2011,
accepted for publication November 24, 2011.)

https://doi.org/10.1017/jmech.2012.51 Published online by Cambridge University Press